Can earthquake swarms trigger the San Andreas fault in the Brawley seismic zone? Continued study of dynamic rupture scenarios in the Salton Trough region.

Report for SCEC Award #17055
Submitted June 15, 2018

Investigators: Christodoulos Kyriakopoulos (UCR), David D. Oglesby (UCR), Thomas K. Rockwell (SDSU) and Aron J. Meltzner (EOS)

I. Project Overview

A. Abstract

We have continued our investigation of multi-fault dynamic rupture scenarios in the Salton Trough, and specifically the Brawley Seismic Zone (BSZ), which has been funded with previous SCEC awards. Our models are based on a postulated fault geometry that includes the extensions of the Southern San Andreas Fault (SSAF) and the Imperial Fault (IF), as well as a system of linking cross-faults (CF) intersecting the SSAF and IF. A significant part of our effort goes into understanding how this system of interconnected faults behaves dynamically. Our previous results have shown that, with our current fault geometry and under the current model assumptions, a through going rupture (either North to South or South to North) in this area is possible. However, many questions remained open regarding the influence of the CF in the overall rupture. In the work summarized in this report, we significantly extended the investigated parameter space to include new rupture scenarios that include a pre-stress contrast between the SSAF-IF and CF, segmented faults, nucleation location near the branch, nucleation on a cross fault, shallower locking depth, and other features. The new experiments are based on a combination of modified fault geometries and different pre-stress conditions. Results from SCEC Award #17055 expanded significantly our understanding of the possible mechanism that could led to a multi fault event and highlighted the importance of dynamic rupture simulations. We were able to verify that if the system of cross-faults is pre-stressed at a higher level than the SSAF-IF main faults (consistent with regional stressing), the cross-faults could modulate the normal stress on the SSAF-IF and provide a mechanism for earthquake termination. We also explored the effect of a shallower locking depth and fault segmentation that proved to be a significant parameter for the propagation of rupture across the BSZ.

B. SCEC Annual Science Highlights

C. Exemplary Figure

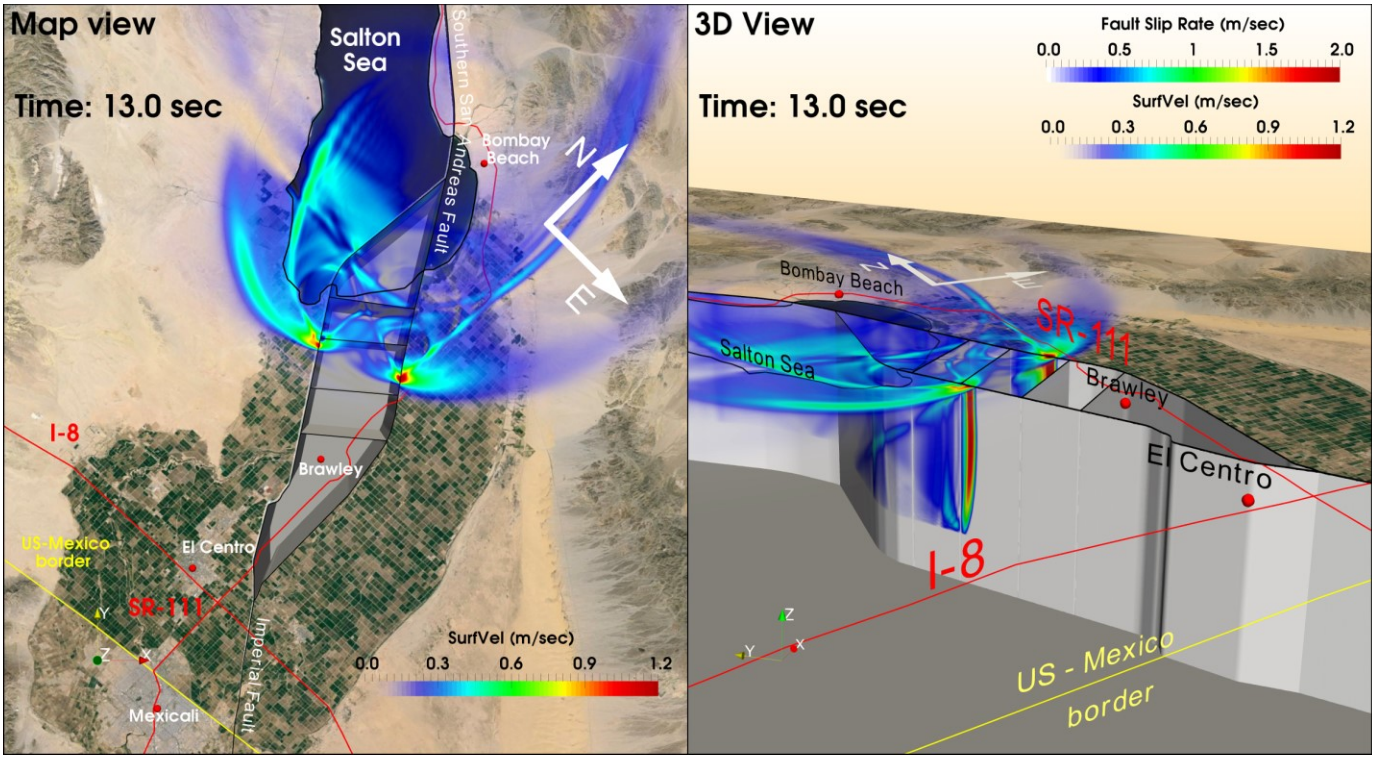

Dynamic rupture model of through-going rupture in the Brawley Seismic Zone. The nucleation location is on the SSAF (North to South propagation). Note how rupture propagates through an area of fault complexity and where the cross-faults intersect the main segments. Interstate I-8 and state highway SR-111 are marked with red lines. The yellow line shows the US-Mexico border. The black thick line represents the Salton Sea shoreline. The dynamic rupture code used for this simulation is FaultMod (Barall,2009). Figures are generated with Paraview (www.paraview.org).

D. SCEC Science Priorities: 1d, 3a, 5b

E. Intellectual Merit

We extended our investigation of possible joint rupture scenarios of the SSAF-IF system and their dynamic behavior when intersected by a system of linking cross-faults. The new experiments include models with a) non-homogeneous initial tractions (pre-stress contrast) between the SSAF-IF and the CF; b) experiments with segmented versions of the SSAF-IF; c) experiments with shallower locking depth (15km); d) experiments with nucleation location near the branches; e) experiments with nucleation on a cross-fault.

F. Broader Impact

Although less studied, the southward extension of the SSAF raises many questions regarding a possible interaction with the IF. A possible scenario involving both these faults could be the one in which a rupture nucleating near Bombay Beach will propagate bilaterally to the north, through the Coachella valley, and to the south into the BSZ and eventually connect with the IF. Such event has the potential to disrupt and damage interstate I-8, considered to be a safe corridor in case of the "big one". Nevertheless, for such a scenario to be possible the hypothetical rupture must travel through the BSZ and successfully overcome the combined effect of possible gaps between the SSAF and IF but also the effect of several cross-faults intersecting the SSAF-IF system. In other words, this type of scenario will probably require the activation of several faults. Our study attempts to throw some light in the dynamic behavior of this system. We conducted an extensive study of parameters we believe might play a role in the final outcome of such event.

G. Project Publications

Our work has been presented at the 2017 AGU fall meeting (oral) and the 2017 SCEC annual meeting (poster). We are writing a paper with a detailed description of our work that will be soon submitted to a peer-reviewed journal.

II. Technical Report

A. Introduction and Background

The Brawley seismic zone (BSZ) is the area separating the southern end of the Southern San Andreas Fault (SSAF) near Bombay Beach and the northern end of the Imperial fault (IF). This is a stepover area with significant fault complexity and where slip is transfered between the SSAF and the IF. Furthermore, the microseismicity in this area highlights a network of interconected cross-faults that apparently intersect the SSAF and IF main structures. Historic ruptures in this area have not exited M_W 6.9 (e.g. 1940 IF event) or smaller. However, displacements measured with paleoseismological techniques suggest that older events might have been even larger. More specifically, anomalously large paleoseismic displacements near the northern tip of the IF (Rockwell et al., 2011, USGS FTR), which are chronologically and stratigraphically indistinguishable from large southern SAF ruptures, pose the question of which faults can rupture together, and what conditions might lead a rupture to jump from one fault to another. In this sense, the Brawley stepover might be an "earthquake gate"—sometimes open and allowing rupture to pass through, but other times not.

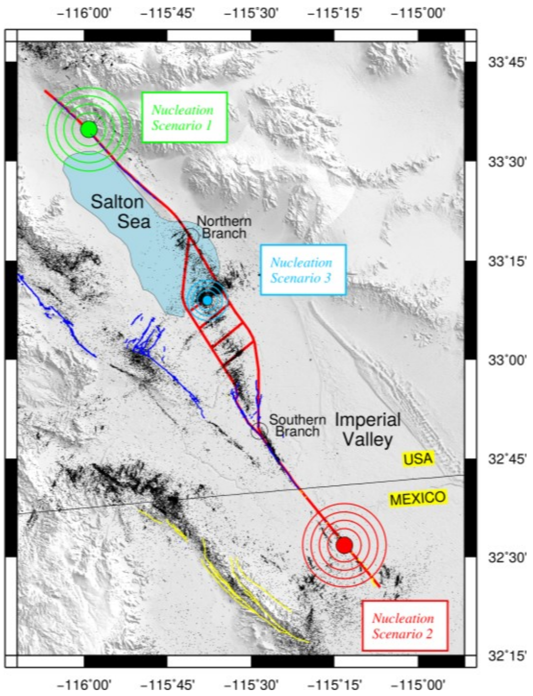

Figure 1. Fault geometry and Nucleation Scenarios. *Our model fault geometry (red line), along with the underlying mapped fault traces (blue curves from USGS) and microseismicity lineaments (black dots) from relocated seismicity of Hauksson et al. (2012).*

B. Method

Using a combination of different datasets, including extensions of mapped fault lines, relocated seismicity catalogues and kinematic constraints, we postulated a system of linking fault structures shown in Figure 1 and 2. This network of faults is implemented in a finite element mesh using Trelis 15.0 (Figure 2). The final mesh includes approximately 80 million hexahedral elements. The mesh density is higher in the volume surrounding the fault network and becomes sparser towards the boundaries of the model domain. The material properties are homogeneous over the entire mesh. See Figure 2 for further details on the finite element mesh. We setup our dynamic rupture simulations using the seismic parameter ***S*** (relative strength) that shows how close to failure is our system. Lower ***S*** values represent a system that is closer to rupture than higher values. We are using the ***S*** value to explore how different pre-stress conditions affect the rupture propagation and the final slip pattern. Specifically, we are testing levels of traction corresponding to S=2.5 (low stress fault), S=2.0 (medium stress fault) and S=0.45 (high stress fault).

$$\boldsymbol{S} = \frac{\tau_{yield}-\tau_{initial}}{\tau_{initial}-\tau_{final}}$$ (Andrews, 1976).

Our multi-fault dynamic rupture simulations are categorized using three first order features: 1) the configuration of the fault system (e.g. continuous versus segmented faults); 2) the initial traction (pre-stress) conditions given by ***S*** of the participating faults; and 3) the nucleation location, on the SSAF (N2S propagation) or IF (S2N propagation) and one experiment with nucleation on a CF. For the computational part of our work we are using the 3D finite element code FaultMod (Barall, 2009). The combination of all the above features resulted in a significant number of simulations. For that reason, we found useful to refer to each model using acronyms that are based on the characteristics mentioned before. For example, a model with nucleation on the SSAF, pre-stress level of S=2.0 on the SSAF and IF, and S=0.45 on the CF, is identified as N2S-S2.0-X0.45. The letter "X" is added to indicate the presence of cross-faults and their corresponding S values and "-14f" the segmented version of the model. That way we achieved a certain level of clarity when discussing the results from each individual model.

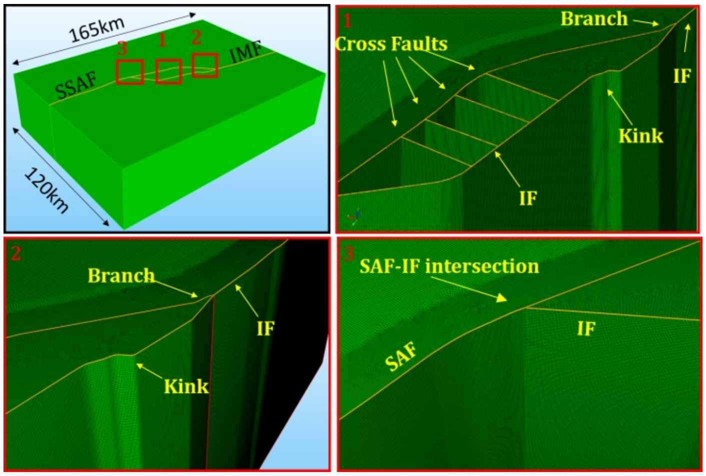

Figure 2. *Fault geometry used in current results. (Top Left panel) Global view of the model domain. The red boxes highlight the areas in panels 1, 2 and 3. (Panel 1) Zoom into the central part of the model hosting the cross faults; (Panel 2) southern IF-SSAF branch; (panel 3) northern SSAF-IF intersection.*

C. Results and Conclusions

The effect of stress heterogeneity--traction contrast--between cross-faults and main segments

Previous results with homogeneous pre-stress conditions across all the faults in the model have shown that under such an assumption the CF have negligible participation in the evolution of rupture. However, in our new experiments we found that the level of participation of the CF in our multi-fault rupture depends on the pre-stress contrast (e.g. CF with S=0.45 and SSAF-IF with S=2.0) between the faults. Specifically, we observed that the CF are more likely to rupture and modulate the normal stress pattern on the SSAF or IF, by increasing the normal stress ahead of the incoming rupture. For example, in the N2S-S2.0-X0.45 case, the southward propagation of rupture is interrupted by the slip on the CF (compare Figure 3E and 3B). Consequently, under certain conditions the cross-faults could provide a stopping mechanism for a through-going rupture.

The effect of fault segmentation

Fault segmentation (implemented as small gaps at the intersections between the SSAF-IF and the CF so that the intersection point is unable to slip in any direction) proved to be a significant stopping mechanism within the framework of our finite element model. Specifically, for models N2S and S2N with S=2.0 the results are significantly different with respect to the original case with continuous faults (e.g. compare Figure 3B to Figure 3F). Fault segmentation was effective in interrupting both S2N and N2S propagating ruptures.

The effect of shallower locking depth

The locking depth in our original simulations is 20 km (e.g. Figure 3B). However, since there is good evidence (Han et al., 2016) suggesting that the crust is thinner beneath the BSZ area, we tested whether a shallower locking depth of 15km (with less seismic moment available; $M_0^{\,20\mathrm{km}} > M_0^{\,15\mathrm{km}}$) reduces the likelihood of rupture propagation (Smith-Konter et al., 2011). We found that in general a 15km locking depth decreases the slip and consequently the concentration of stress at the rupture front is lower. More specifically, for S2.0 models and higher, this effect largely prevents rupture propagation onto the IF (N2S case, Figure 3H) or SSAF (Figure 3I, S2N case) in the area in which they overlap.

The effect of nucleation near the branches

The nucleation location in our main experiments occurs at approximately 30km from either the north or south branch. However, we wanted to test what could be the effect of a nucleation location near the southern branch (e.g. similarly to the Mw 6.9 1940 Imperial Valley event). For S=2.5 the result appears very similar to the original if we account for the expected shift of the high slip area around the nucleation zone. For S=2.0, the most notable difference is the absence of of slip on the IF, most probably do due to the reduced directivity.

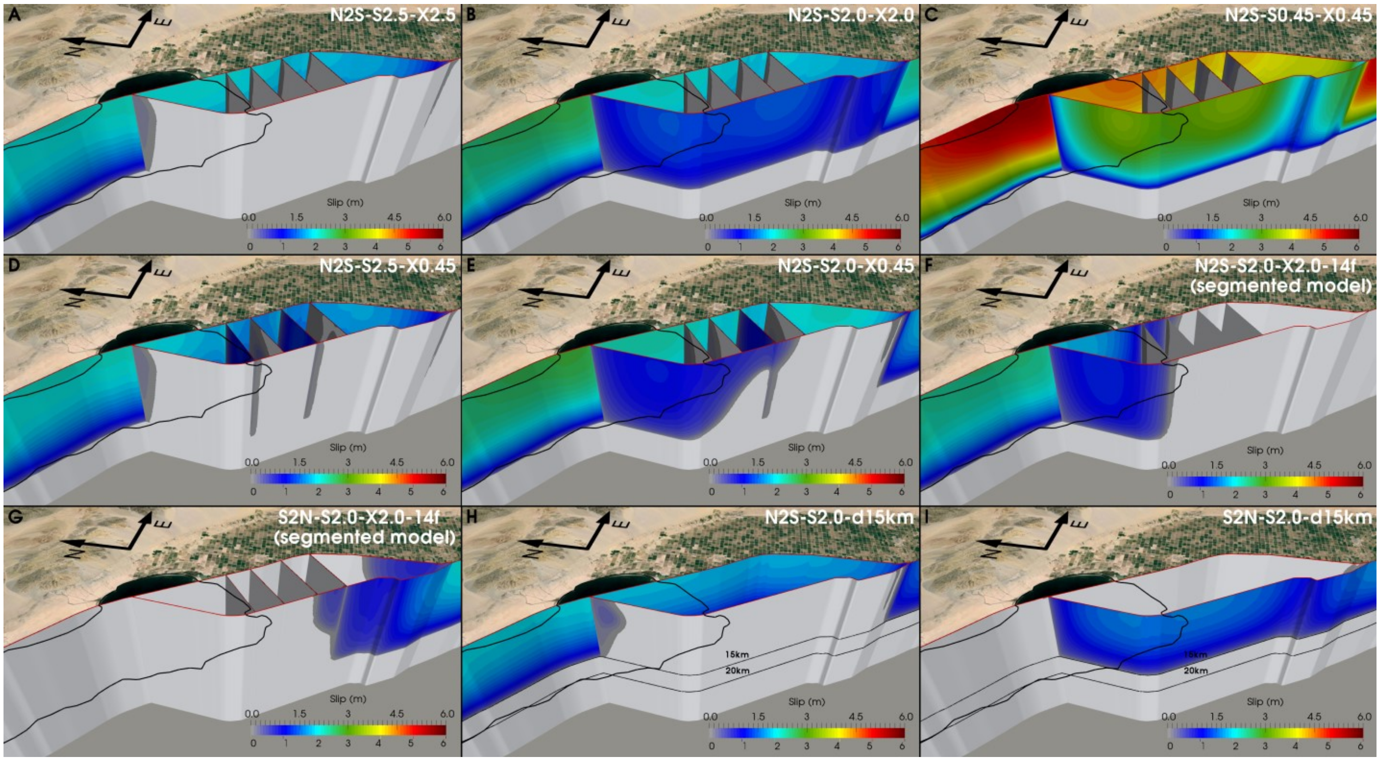

Figure 3. *Final slip distribution for dynamic rupture models. (A), (B) and (C) show simulations with homogeneous pre-stress in all the participating faults, S=2.5 (low stress), S=2.0 (medium stress) and S=0.45 (high stress) respectively. (D) Simulation with S=0.45 on the cross faults and 2.5 on the SSAF-IF (N2S-S2.5-X0.45); (E) same as (D) but S=2.0 on SSAF-IF (N2S-S2.0-X0.45); (F) segmented model with nucleation on SSAF (N2S-S2.0-X2.0-14f); (G) same as (F) but with nucleation on IF; (H) and (I) models with 15km locking depth, S=2.0 in SSAF-IF, and nucleation on the SSAF and IF respectively.*

Triggering of the SSAF by “swarm” type medium size earthquakes on cross-faults

How large and how close to the SSAF must be a cross-fault event to trigger a larger (“the big one”) Southern San Andreas event? To answer this question, we tested cross-fault earthquake scenarios with two different nucleation locations: a) at the center of the cross-fault; and b) at the edge of the cross-fault (immediately adjacent to the SSAF).

Both the epicenters are at 6km depth. The size of the events, ~M5 up to M6, is modulated by altering the allowed area of rupture on the cross-fault (with the main fault free to rupture). Results of the two experiments are shown in Figure 4. Based on the simulations with our current fault geometry and with the assumed model parameters, we observe the following: 1) a medium-size event (~M5.5; consistent with the observed magnitude of swarm earthquakes in this region) nucleating immediately adjacent to the SSAF is able to trigger a major event on the SSAF; 2) An event of the same size as (1) and nucleating in the center of the CF does not produce enough stress transfer to the SSAF to trigger it and cascade into a larger earthquake. This latter effect is similar to that observed in the 2012 Brawley swarm (Hauksson et al., 2017), in which an M 5.5 event did not trigger the SSAF. This observation may imply that the event took place on a cross-fault far from the SSAF junction, or that the SSAF does not extend far enough south to intersect the cross-fault. A comprehensive evaluation of rupture initiation on cross-faults, including transfer onto the SSAF, requires a more accurate description of the earth medium.

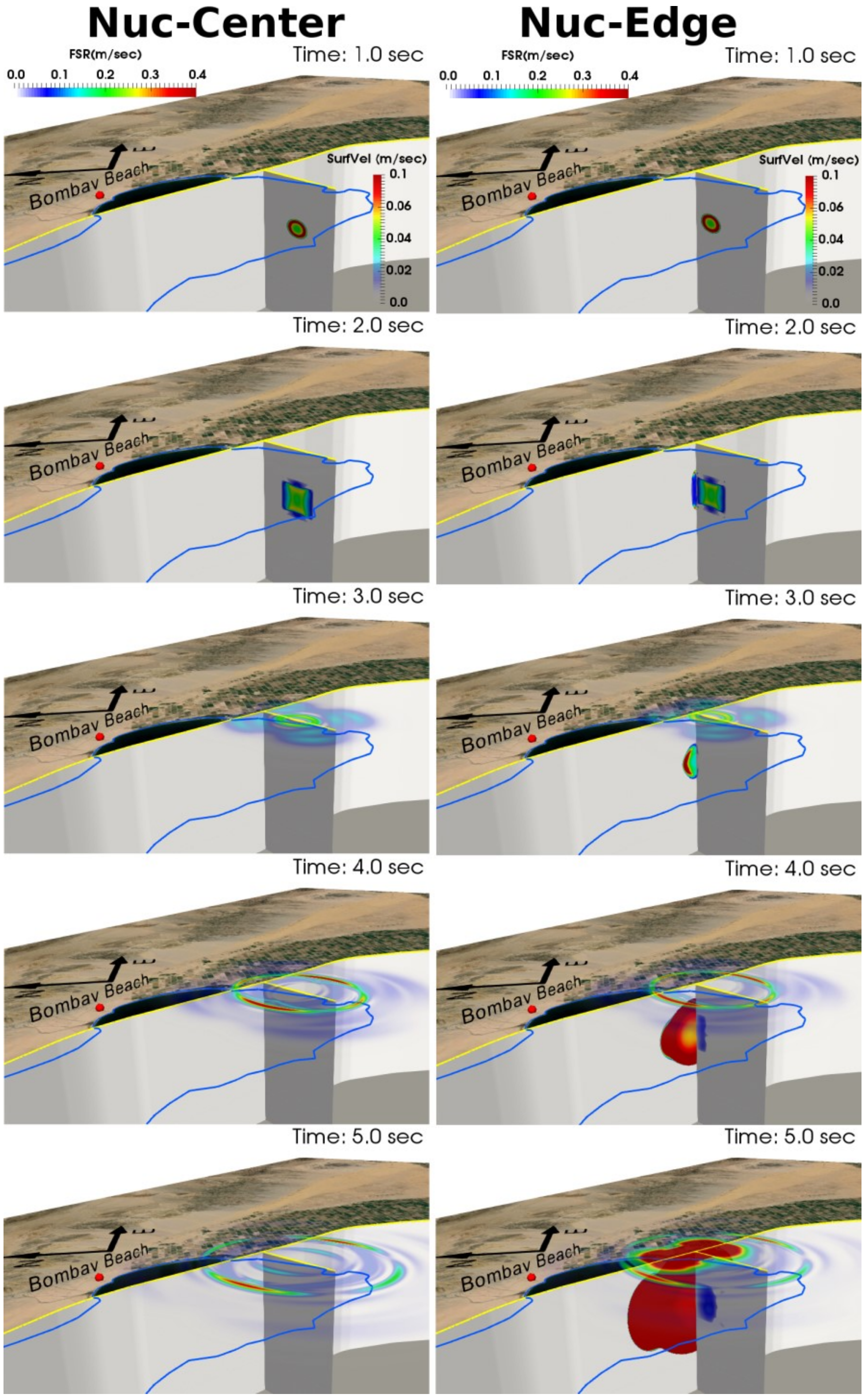

Figure 4. Triggering of the SSAF by a cross-fault earthquake. Snapshots of fault slip rate. *(Left column) Model with nucleation at the center of the cross-fault. Rupture start and dies on the CF without propagating on the SSAF. (Right column) Model with nucleation adjacent to the SSAF. Here rupture on the CF becomes the initiation phase of a large SSAF event. To improve the visual effect, we also show in both panels the surface particle velocity (m/sec). The blue line highlights the Salton Sea shoreline.*

References Cited

Andrews D.J, (1976), Rupture propagation with finite stress in antiplane strain, J. Geophys. Res. Solid Earth, 81, 3575-3582

Barall, M., (2009). A grid-doubling technique for calculating dynamic three-dimensional rupture on an earthquake fault, *Geophysical Journal International*, 178, 845-859, doi:10.1111/j.1365-246X.2009.04190.x.

Han, L., et al. (2016), Continental rupture and the creation of new crust in the Salton Trough rift, Southern California and northern Mexico: Results from the Salton Seismic Imaging Project, J. Geophys. Res. Solid Earth, 121, 7469–7489, doi:10.1002/2016JB013139.

Hauksson, E., M.-A. Meier, Z. E. Ross, and L. M. Jones (2017), Evolution of seismicity near the southernmost terminus of the San Andreas Fault: Implications of recent earthquake clusters for earthquake risk in southern California, Geophys. Res. Lett., 44, 1293–1301, doi:10.1002/2016GL072026.

Janecke, S.U. and Markowski, D.K., 2013 (2016 revised), Revised SCEC Final report on the East Shoreline strand of the San Andreas fault: SCEC database http://scecinfo.usc.edu/core/cis/list_reports.php 170 p.

Rockwell, T.K., Meltzner, A., Tsang, R. (2011). A long record of earthquakes with timing and displacements for the Imperial fault: A test of earthquake recurrence models. Technical Report. U.S. Geological Survey.

Smith-Konter, B. R., D. T. Sandwell, and P. Shearer (2011). Locking depths estimated from geodesy and seismology along the San Andreas Fault System: Implications for seismic moment release, J. Geophys. Res., 116, B06401, doi:10.1029/2010JB008117.